

Hysteresis Modelling in Electromechanical Transducer with Magnetic Shape Memory Alloy

Abstract. The article presents a new class of smart materials which are magnetic shape memory alloys. These alloys combines both good dynamics and large strains. These properties make it possible to use these materials in positioning transducers which are alternative for classical electromagnetic transducers such as proportional solenoids. Unfortunately as other smart materials, MSMA are distinguished by hysteresis phenomenon which loop in this case is very wide and asymmetric. Authors present result of strain measurement which was performed for decreasing amplitude sine input signal. Based on this result phenomenological generalized Prandtl-Ishlinskii model was matched and compared.

Streszczenie. Artykuł zawiera opis nowej grupy materiałów inteligentnych, jaką są materiały z magnetyczną pamięcią kształtu. Materiały te łączą w sobie dobre właściwości dynamiczne oraz duży zakres możliwych odkształceń. Właściwości te powodują, iż istnieje realna szansa na praktyczną ich aplikację w konstrukcji przetworników pozycjonujących, które mogą konkurować z rozwiązaniami klasycznymi np. elektromagnesami proporcjonalnymi. Autorzy zaprezentowali wynik pomiaru wydłużenia dla gasnącej amplitudy sinusoidalnego sygnału sterującego. Na podstawie zarejestrowanych wyników dopasowano do nich uogólniony fenomenologiczny model histerezy Prandtla-Ishlińskiego oraz dokonano porównania. (Modelowanie histerezy w elektromechanicznym przetworniku z materiałem z magnetyczną pamięcią kształtu)

Keywords: hysteresis, Prandtl-Ishlinskii model, magnetic shape memory alloy, asymmetric hysteresis

Słowa kluczowe: histereza, model Prandtla-Ishlińskiego, stopy z magnetyczną pamięcią kształtu, histereza asymetryczna

doi:10.12915/pe.2014.11.62

Introduction

In the area of devices which are classified in a group of precise mechanics and in systems where very high operating accuracies are required, for example in positioning actuators with maximum error not bigger than few micrometres electromagnetic transducers are used. Main task of such transducers is conversion of electrical input signal in to non-electrical output signal (force, pressure, flow rate, displacement). Development and increasing needs especially in bioengineering, aerospace, marine and military engineering forced scientists to search for new unconventional solutions. Active materials (smart materials), are able to fulfil needs such as reduction of mass and production costs, while improving the most important operating parameters (dynamics, accuracy). Smart materials usually change their shape under external stimulus (electric and magnetic field, temperature)[1, 2, 3].

Common feature of these materials is occurrence of nonlinearities such as hysteresis phenomenon which strongly disturbs precise positioning. Systems with smart materials can be controlled in closed loop. Unfortunately this solution is very expensive (cost of high precision sensors), and sensor in itself can be very big compared to transducer size. Other way is adaptation of inverse hysteresis model to control system, which can compensate in real time this nonlinearity. One of well-known phenomenological models can be applied (e.g. Prandtl-Ishlinskii, Krasnosel'skii-Pokrovskii, Preisach), which are widely described in literature [4, 5]. Classical Prandtl-Ishlinskii model describes only hysteresis which is distinguished by symmetric loop. Modifications allow also for modelling asymmetric loops distinguished for magnetostrictive and shape memory alloys [5,6,7].

Magnetic shape memory materials

Group of smart materials which change their properties in external magnetic field (magnetostrictive materials and magnetorheological fluids), since 1996 has expanded to materials with magnetic shape memory. This interesting and promising material was described by Ullakko [8]. Due to high dynamics (1÷2 kHz), and large possible strains up to 10%, magnetic shape memory alloys are next active materials with possibility of practical applications in positioning systems. These materials have a chance to fill a gap between thermal activated shape memory alloys and magnetostrictive materials [9]. The most popular alloy is

composition of nickel, manganese and gallium (Ni_2MnGa), with 6% of maximum strain. This material is distinguished by low relative magnetic permeability, for this reason one side in sample is clearly shorter than other. That shape reduces size of magnetic core and coil turns.

Design of examined transducer is based on spring returned operating mode available for MSM materials. This mode is one of five possible, which are detailed described in [10]. The biggest disadvantage of this mode is necessity of compressive force generation. The most popular mechanism is front placed coil spring which is pretensioned (Fig. 1). Unfortunately this tension causes that blocking force is reduced two times and maximum strain decreases with it. Narrower strain range appears because compressive force is not sufficiently large to provide crystal lattice reorientation which was deformed in magnetic field thus that after first cycle maximum strain is reduced.

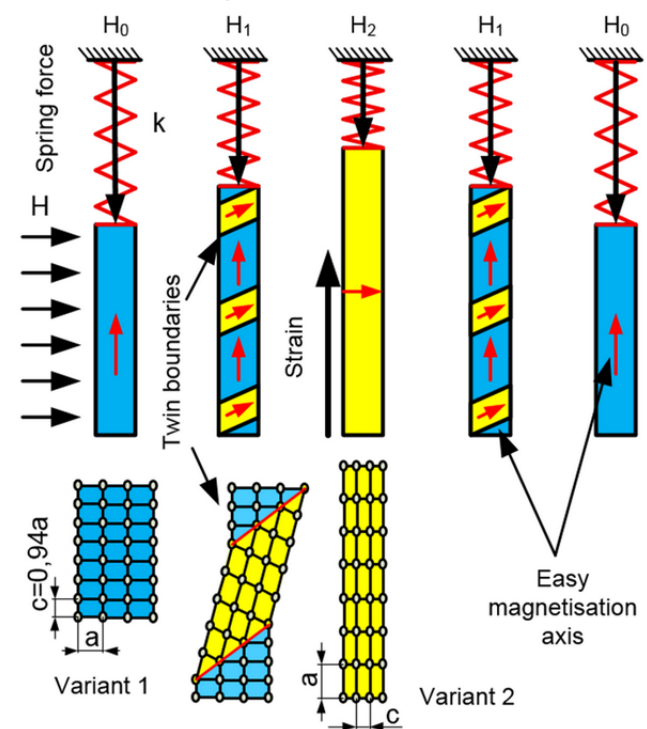


Fig. 1. Spring returned operating mode

Increasing strength of external magnetic field causes reorientation between martensite variants (Fig. 1). As a result of this movement volume of variant 2 raises at the expense of variant 1. Shorter lattice side (c), is placed parallel to strain direction and to easy magnetization axis. Such properties are obtained in production process. When material is cooling very accurate compressive force is applied. Without external magnetic field magnetic vectors are arranged along easy magnetization axis. Raising magnetic field (perpendicular to easy axis), causes rotation of these vectors according to direction of this field. If crystal lattice reorientation energy is sufficiently smaller than magnetocrystalline anisotropy energy then lattice rotates with magnetic vector. This rotation occurs at twin boundaries, after rotation easy magnetization axis is arranged parallel to direction of magnetic field [2].

Hysteresis phenomenon in MSM materials

Very big disadvantage of magnetic shape memory alloys is wide hysteresis loop for both characteristics strain vs. current and force vs. current [11, 12] (Fig. 2.). This nonlinearity has mainly drawbacks, but also advantages should be mentioned. Main cause of such behaviour is occurrence of twinning stress in crystal lattice, which is a kind of internal friction. Material for magnetic core is also important, but in this case magnetic hysteresis can be reduced by application of proper materials and heat treatment such as annealing. Due to twinning stress MSM effect is self-supporting. Sample elongated in magnetic field remains in this form until external force does not exceed lattice friction. It is very useful effect in damping reduction applications but when it is a need for micro positioning hysteresis strongly hinders this process (causing oscillations and inaccuracy) [6, 10, 13].

In literature good and reliable analysis of different control strategies and hysteresis modelling (Krasnosel'skii-Pokrovskii model), in MSM materials shows paper [14]. Another examples of hysteresis modelling which includes influence of operating temperature can be found in [15, 16].

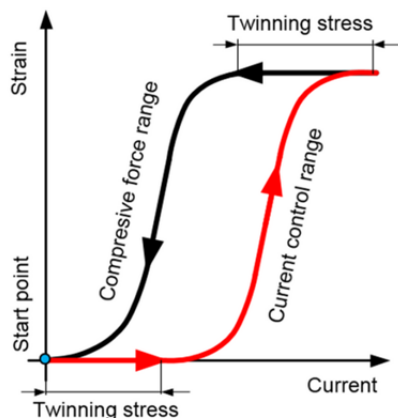


Fig. 2. Example strain vs current curve with hysteresis in MSM materials

Prandtl-Ishlinskii hysteresis model

This part of publication describes generalized Prandtl-Ishlinskii (GPI), which is one of well-known phenomenological hysteresis models. Classical Prandtl-Ishlinskii model (PI), is proper for description of symmetric hysteresis loops just like in piezo based transducers. On the other hand transducers based on magnetostrictive or shape memory alloys (both magnetic and thermal), show high degree of asymmetry and saturation in hysteresis loops. For this purpose modification in syntax of hysteresis PI model was proposed [13, 17, 18, 19]. Based on mentioned papers Authors endeavoured to use generalized PI model for

hysteresis modelling in MSM based transducer. Generalized PI model have not been considered for MSM transducers so far.

Classical PI hysteresis model is a superposition of single play operators, which output value unlike Preisach and Krasnosel'skii-Pokrovskii relay operators can be greater than $(-1,1)$. Play operator which is shown in figure 3 is distinguished by input v and threshold r which gives width of this operator.

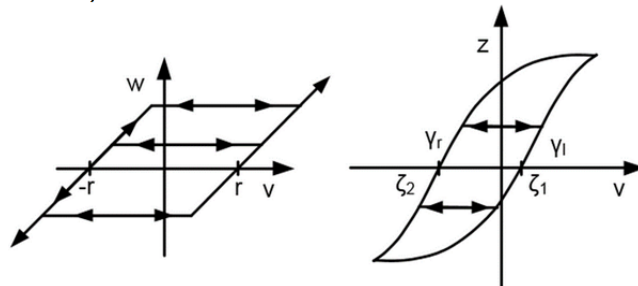


Fig. 3. Classical PI play operator (left), generalized play operator (right)

Play operator F_r behaves like backlash block in Simulink. Backlash block represents equal proportional change in output for raising input. Implicitly in backlash when threshold equals 0 output value is given by $f(x)=x$ function. This discontinuity works when input changes direction, then decreasing input does not change output value e.g. gear boxes mechanism or screw drives. Output value F_r can be described as formulation (1) for input function $v(t)$ which is monotone in each subinterval $[t_i, t_{i+1}]$ and satisfies conditions (2)(3). These conditions are also true for generalized output G_r . Dependence between input and output value of this model is represented by equation (4). Each output of single play operator is multiplied by $p(r)$ which is non-negative density function determined from measured input-output transducer characteristics [18].

$$(1) \quad F_r[v](t) = \begin{cases} \max(v(t) - r, w(t_i)), & \text{for } v(t) > v(t_i) \\ \min(v(t) + r, w(t_i)), & \text{for } v(t) < v(t_i) \\ w(t_i), & \text{for } v(t) = v(t_i) \end{cases}$$

$$(2) \quad t_i < t \leq t_{i+1}$$

$$(3) \quad 0 < i \leq N - 1$$

$$(4) \quad Y_p(t) = \omega(v)[t] + \int_0^R p(r) F_r[v](t) dr$$

In generalized operator output value G_r increases along function defined as γ_l and decreases along other γ_r (5). This combination helps in description of asymmetric behaviour.

$$(5) \quad G_r[v](t) = \begin{cases} \max(\gamma_l(t) - r, z(t_i)), & \text{for } v(t) > v(t_i) \\ \min(\gamma_r(t) + r, z(t_i)), & \text{for } v(t) < v(t_i) \\ z(t_i), & \text{for } v(t) = v(t_i) \end{cases}$$

For description of generalized play operator two envelop functions are used. These functions are based on hyperbolic tangent function which allows for description of saturation.

$$(6) \quad \gamma_r = a_0 \tanh(a_1 v + a_2) + a_3$$

$$(7) \quad \gamma_l = b_0 \tanh(b_1 v + b_2) + b_3$$

Density function is different for each play operator and depends on threshold value. Value of r_j is always positive and N is number of generalized play operators. In this case twelve operators were used.

$$(8) \quad p(r_j) = \rho e^{-\tau r_j}$$

$$(9) \quad r_j = \alpha j$$

$$(10) \quad j \in \{1; N\}$$

Sum of integral generalized operator and value of function $\Omega[v](t)$ (11) is an output of model. Described integral can be also represented by sum of finite number of generalized play operators (12).

$$(11) \quad Y_{PY}(t) = \Omega[v](t) + \int_0^R p(r)G_{lr}^Y[v](t)dr$$

$$(12) \quad Y_{PY}(t) = \Omega[v](t) + \sum_{j=1}^N p(r_j)G_{l_j r_j}^Y[v](t)dr$$

Function $\Omega[v](t)$ consists two different hyperbolic tangent functions which act separately for increasing and decreasing input signal. Similar analysis shows paper [20].

$$(13) \quad \Omega[v](t) = \begin{cases} c_0 \tanh(c_1 v + c_2) + c_3 & \text{for } \frac{dv}{dt} \geq 0 \\ d_0 \tanh(d_1 v + d_2) + d_3 & \text{for } \frac{dv}{dt} < 0 \end{cases}$$

Test bench

Prepared test bench consists: PC computer with Matlab Simulink (no. 3) and dSPACE Control Desk, which was used as control and data acquisition system (no. 2, 4). Outputs module DAC was connected with laboratory programmable DC power source with range: 0÷32 V, 0÷10 A (no. 5). Output voltage and current are set by voltage control signal from DAC card (0÷10 V). Magneto motive force was generated by two coils. These coils were connected parallel, excitation current was 5 A. Maximum magnetic induction measured in 1.2 mm width air gap was 0.7 T. Magnetic core was made of typical construction steel S215. Stiffness of returning spring is 0.43 N/mm. Magnitude of prestress was set by table with micrometre screw (no. 1). For research purpose sample 1x2.5x20 mm was used. Detailed description of MSMA transducer and previous research were placed in [11, 12].

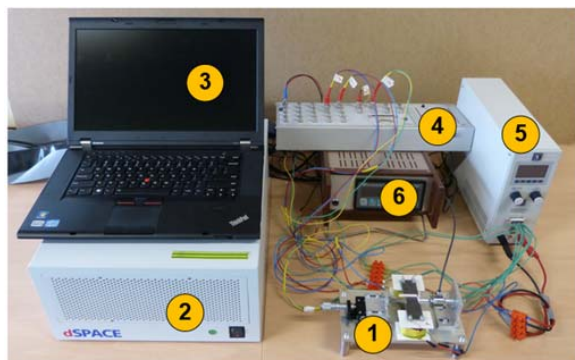
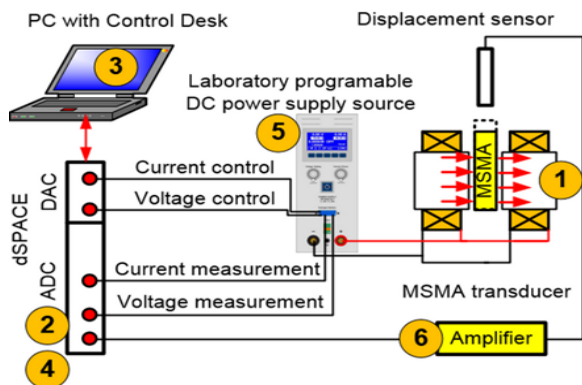


Fig. 4 Scheme of test rig

Results

First step of modelling was measurement on aforementioned test bench. As an input signal sine wave was used, which is described by function (14).

$$(14) \quad v(t) = A \sin(f \cdot t + k\pi) + v'$$

where A is amplitude, f is frequency, v' is function bias. Values of each parameter are given in equation (15).

$$(15) \quad v(t) = \begin{cases} 0 & \text{for } t \in (0; 10) \\ 2.5 \sin\left(0.2\pi \cdot t - \frac{\pi}{2}\right) + 2.5 & \text{for } t \in (10; 70) \end{cases}$$

Amplitude of input signal is asymptotically decreasing to line at 2.5 A. Decreasing starts at 20 second (16)(17).

$$(16) \quad V(t) = \begin{cases} v(t) & \text{for } t \in (0; 20) \\ v(t) \cdot (1 - 0.01 \cdot q(t)) & \text{for } t \in (20; 70) \end{cases}$$

$$(17) \quad q(t) = t - 20 \quad \text{for } t \in (20; 70)$$

Input signal is plotted in figure 5. The same signal was used in simulation model. For parameters estimation non-linear least squares method was used. Results of estimation are placed in Table 1. Comparison of results obtained in estimated model and measurement are plotted in figure 6. Next figure 7 shows how maximum error changes with time. The most important graph is figure 8. In this figure hysteresis loops are plotted as a function of input current.

Table 1. Estimated parameters for MSMA transducer

Parameter	Estimated values [dimensionless]
α	-0.1993
ρ	5.6438
τ	0.0714
a_0	8.5043
a_1	0.5140
a_2	-0.0612
a_3	-6.1533
b_0	3.3505
b_1	1.3916
b_2	-0.9146
b_3	3.6876
c_0	1.5687
c_1	6.6176
c_2	-11.5359
c_3	25.7303
d_0	2.1349
d_1	7.1117
d_2	-9.2777
d_3	28.1546

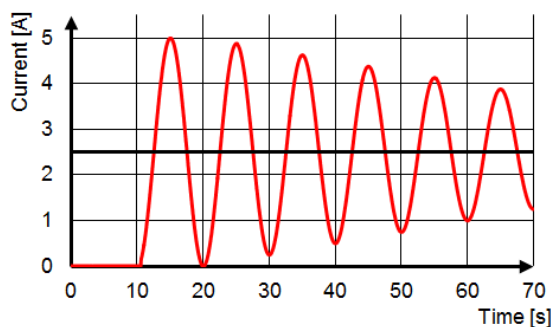


Fig. 5. Input signal

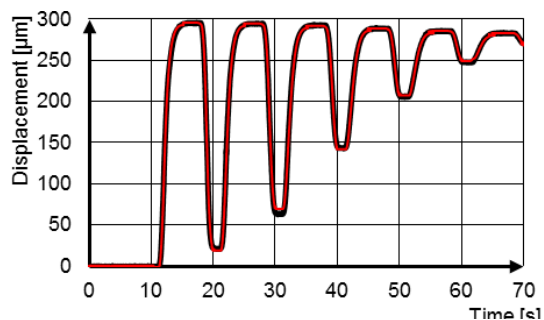


Fig. 6. Displacement vs. time (black line – measurement result, red line – simulation model)

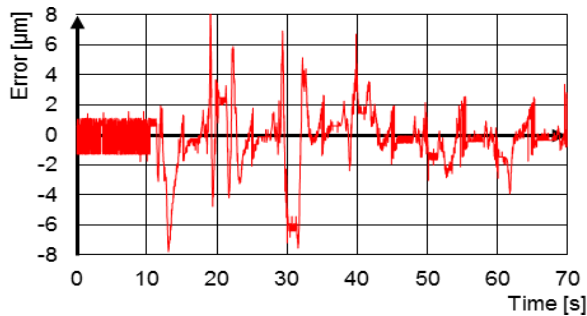


Fig. 7. Model error vs. time

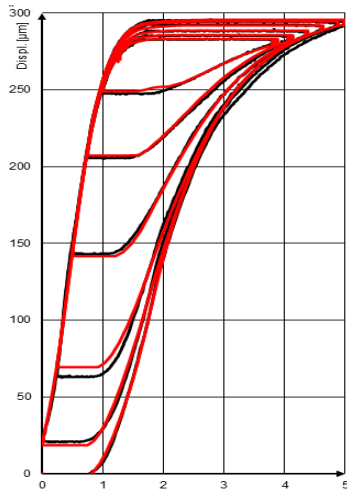


Fig. 8. Displacement vs. current (black line – measurement result, red line – simulation model)

Conclusions

It is worth noticing that the transducer hysteresis is relatively wide and asymmetric, which impede modelling and adaptation process of this phenomenon. However the validation of the MSMA based electromechanical transducer hysteresis model was successful. As shown in figure 8, the model output covers well the measured characteristic. Model error presented in figure 7 has maximal value less than 3% relative to maximal transducer displacement. Error in first 10 seconds of acquisition comes from measurement apparatus noise, when the transducer is not energised and the model output is 0. It indicates what the noise level is during measurements and that real model error could be slightly smaller than value calculated. Important is that the error peaks occurs for input signal returns, especially for local minimums, but these are always difficult to model properly.

Height of figure 8 has been set deliberately. Smaller plot shows that estimation is fully correct and model fits perfect to measurement. Thanks to this representation it can be easily notice where model has differences regarding to real results.

REFERENCES

- [1] Lagoudas D. C., Shape memory alloys: modeling and engineering applications, Springer, Berlin (2008)
- [2] Jokinen T., Ullakko K., Suorsa I., Magnetic Shape Memory materials-new possibilities to create force and movement by magnetic fields, Proceedings of the Fifth Int. Conference on Electrical Machines and Systems ICEMS, (2001), 20-23
- [3] Meier H., Czechowicz A., Haberland C., Langbein S., Smart control systems for smart materials, Journal of materials engineering and performance, 20 (2011), No. 4-5, 559-563
- [4] Kuhnen K., Modeling, identification and compensation of complex hysteretic nonlinearities: A modified Prandtl-Ishlinskii approach, European J. of Control, 9 (2003), No. 4, 407-418
- [5] Riccardi L., Naso D., Turchiano B., Janocha H., Robust adaptive control of a magnetic shape memory actuator for

- precise positioning, American Control Conference, San Francisco (USA), 2011, 5400-5405
- [6] Riccardi L., Naso D., Turchiano B., Janocha H., Adaptive approximation-based control of hysteretic unconventional actuators, 50th IEEE Conference on Decision and Control and European Control Conference CDC-ECC, (2011), 958-963
- [7] Riccardi L., Naso D., Turchiano B., Janocha H., Palagachev D. K., On PID control of dynamic systems with hysteresis using a Prandtl-Ishlinskii model, IEEE Conference on American Control Conference ACC, (2012), 1670-1675
- [8] Ullakko K., Huang J. K., Kantner C., O'Handley R. C., Kokorin V. V., Large magnetic-field-induced strains in Ni₂MnGa single crystals, Applied Physics Letters, 69 (1996), No. 13, 1966-1968
- [9] Mohd Jani J., Leary M., Subic A., Gibson M. A., A review of shape memory alloy research, applications and opportunities, Materials & Design, 56 (2014), 1078-1113
- [10] Holz B., Riccardi L., Janocha H., Naso D., MSM actuators: design rules and control strategies, Advanced Engineering Materials, 14 (2012), No. 8, 668-681
- [11] Minorowicz B., Nowak A., Stefański F., Position regulation of magnetic shape memory actuator, J. of Achievements in Materials and Manufacturing Eng. 61 (2013), No. 2, 216-221
- [12] MINOROWICZ B., NOWAK A., Force generation survey in magnetic shape memory alloys, Archives of Mechanical Technology and Automation, 33 (2013), No. 1, 37-46
- [13] Al Janaideh M., Rakheja S., Su C.-Y., An analytical generalized Prandtl-Ishlinskii model inversion for hysteresis compensation in micropositioning control, IEEE/ASME Transactions on Mechatronics, 16 (2011), No. 4, 734-744
- [14] Riccardi L., Naso D., Janocha H., Turchiano B., A precise positioning actuator based on feedback-controlled magnetic shape memory alloys, Mechatronics, 22 (2012), No. 5, 568-576
- [15] Schlüter K., Riccardi L., Raatz A., An Open-Loop Control Approach for Magnetic Shape Memory Actuators Considering Temperature Variations, Advances in Science and Technology, 78 (2013), 119-124
- [16] Riccardi L., Naso D., Turchiano B., Janocha H., Adaptive control of positioning systems with hysteresis based on magnetic shape memory alloys, IEEE Transactions on Control Systems Technology, 21 (2013), No. 6, 2011-2023
- [17] Al Janaideh M., Su C.-Y., Rakheja S., Development of the rate-dependent Prandtl-Ishlinskii model for smart actuators, Smart Materials and Structures, 17 (2008), No. 3, 035026
- [18] Al Janaideh M., Rakheja S., Su C.-Y., A generalized Prandtl-Ishlinskii model for characterizing the hysteresis and saturation nonlinearities of smart actuators, Smart Materials and Structures, 18 (2009), No. 4, 045001
- [19] Al Janaideh M., Rakheja S., Mao J., Su C.-Y., Inverse generalized asymmetric Prandtl-Ishlinskii model for compensation of hysteresis nonlinearities in smart actuators, International Conference on Networking, Sensing and Control ICNSC'09, (2009), 834-839
- [20] Flaga S., Oprzędkiewicz I., Sapiński B., Characteristics of an experimental MSMA-based actuator, Solid State Phenomena, 198 (2013), 283-288



Acknowledgements

M.Sc. Bartosz Minorowicz is a scholar within Sub-measure 8.2.2 Regional Innovation Strategies, Measure 8.2 Transfer of knowledge, Priority VIII Regional human resources for the economy Human Capital Operational Programme Co-financed by European Social Fund and state 02/22/DSPB/1145

Authors:

Corresponding author:

M.Sc. Eng. Bartosz Minorowicz,

E-mail: bartosz.minorowicz@gmail.com

M.Sc. Eng. Amadeusz Nowak,

E-mail: nowak.amdeusz@gmail.com

M.Sc. Eng. Frederik Stefański,

E-mail: frederik.stefanski@gmail.com

Poznan University of Technology, Division of Mechatronics Devices, Piotrowo Street 3, 60-695 Poznan, Poland